Journal of Orthopaedic Surgery and Research

RESEARCH ARTICLE

Open Access

A comparative study of the effect of facet tropism on the index-level kinematics and biomechanics after artificial cervical disc replacement (ACDR) with Prestige LP, Prodisc-C vivo, and Mobi-C: a finite element study

Jing Li[1†], Ye Li[2†], Junqi Zhang[1], Beiyu Wang[1], Kangkang Huang[1], Hao Liu[1] and Xin Rong[1*]

Abstract

Introduction Artificial cervical disc replacement (ACDR) is a widely accepted surgical procedure in the treatment of cervical radiculopathy and myelopathy. However, some research suggests that ACDR may redistribute more load onto the facet joints, potentially leading to postoperative axial pain in certain patients. Earlier studies have indicated that facet tropism is prevalent in the lower cervical spine and can significantly increase facet joint pressure. The present study aims to investigate the changes in the biomechanical environment of the cervical spine after ACDR using different prosthese when facet tropism is present.

Methods A C2-C7 cervical spine finite element model was created. Symmetrical, moderate asymmetrical (7 degrees tropism), and severe asymmetrical (14 degrees tropism) models were created at the C5/C6 level by adjusting the left-side facet. C5/C6 ACDR with Prestige LP, Prodisc-C vivo, and Mobi-C were simulated in all models. A 75 N follower load and 1 N·m moment was applied to initiate flexion, extension, lateral bending, and axial rotation, and the range of motions (ROMs), facet contact forces(FCFs), and facet capsule stress were recorded.

Results In the presence of facet tropism, all ACDR models exhibited significantly higher FCFs and facet capsule stress compared to the intact model. In the asymmetric model, FCFs on the right side were significantly increased in neutral position, extension, left bending and right rotation, and on both sides in right bending and left rotation compared to the symmetric model. All ACDR model in the presence of facet tropism, exhibited significantly higher facet capsule stresses at all positions compared to the symmetric model. The stress distribution on the facet surface and the capsule ligament in the asymmetrical models was different from that in the symmetrical model.

[†]Jing Li and Ye Li contributed equally to this work.

*Correspondence:
Xin Rong
rongxin@scu.edu.cn

Full list of author information is available at the end of the article

Conclusions The existence of facet tropism could considerably increase FCFs and facet capsule stress after ACDR with Prestige-LP, Prodisc-C Vivo, and Mobi-C. None of the three different designs of implants were able to effectively protect the facet joints in the presence of facet tropism. Research into designing new implants may be needed to improve this situation. Clinical trials are needed to validate the impact of facet tropism.

Keywords Facet tropism, Artificial cervical disc replacement, Facet joint, Biomechanics, Finite element

Introduction

Artificial cervical disc replacement (ACDR), as a conventional surgical approach for treating cervical spine conditions, has been widely performed and has demonstrated positive clinical outcomes [1–5]. However, research has revealed that approximately 17.2% of patients undergoing ACDR experience postoperative axial pain [6], which can reduce overall satisfaction with the surgery. Current research suggests that several clinical factors can influence postoperative axial pain in cervical spine surgeries, including age, preoperative axial pain, variations in surgical techniques, and postoperative management. Changes in the biomechanical environment of the facet joints after surgery may be one of the contributing factors to postoperative axial pain [6, 7]. Some studies have indicated that ACDR can potentially alter load distribution within the facet joints [7, 8], which may be one of the reasons behind the occurrence of postoperative axial pain following ACDR.

Facet tropism refers to the absolute difference in tilt angles between the facet joints on both sides of the same segment. Earlier research has shown that facet tropism is commonly found in the lower cervical spine (18–25%) and leads to a significant increase in facet contact forces (FCFs) [9–12]. The intervertebral disc, along with the bilateral facet joints posteriorly, forms a three-joint complex. The three joints within each motion segment are highly interdependent [13, 14]. When facet tropism is present, the tilting of the three-joint complex may significantly alter the biomechanical environment of the spine. This can also lead to changes in how various implant designs affect the facet joints.

Finite element analysis (FE) is an effective method for evaluating the biomechanics of the spine after surgery or in special circumstances [9, 15, 16]. Previous FE studies have explored the biomechanical effects of ACDR and the impact of different implants on spine biomechanics [8, 17, 18]. However, most current FE research primarily focuses on analyzing the biomechanical effects of ACDR or different implants in normal anatomical conditions, with limited reporting on the biomechanical effects of ACDR in the presence of facet joint structural abnormalities. In this study, we established FE models for three commonly used but design different artificial intervertebral discs—Prestige-LP, Prodisc-C Vivo, and Mobi-C—under varying facet joint symmetry conditions by altering implant and facet joint surface angles to investigate the changes in the biomechanical environment of the cervical spine after ACDR using different prosthese when facet tropism is present. To our knowledge, this represents the first study examining the postoperative biomechanical environment of ACDR in the context of anatomical structural abnormalities.

Materials and methods

Intact models

We used a CT scanner (SOMATOM Definition AS+, Siemens, Germany) to scan a 28-year-old male healthy volunteer (165 cm, 65 kg) who signed the informed consent form to participate in this study. The slice thickness was 0.75 mm, and the slice increment was 0.69 mm. The obtained data in DICOM format was loaded into the Mimics 21.0 software (Materialize Inc, Leuven, Belgium), where the C2-T1 vertebrae were reconstructed by thresholding and dynamic region growing. First, the reconstructed cervical spine model was divided into two equal parts along the mid-sagittal plane, with the left half mirrored to create a symmetrical model. Following this, we developed moderate and severe asymmetric models. Using the C5/6 facet joints of the existing symmetrical model as a reference, we established a datum plane. We then simulated the fusion of the bilateral facet joints, maintaining one side of the datum plane unchanged while adjusting the angle of the other side along the sagittal plane(the adjusted facet in this study is the left facet joint), resulting in angular differences of 7 degrees and 14 degrees between the two datum planes. We subsequently utilized these datum planes to partition both sides of the facet joints, generating moderate and severe asymmetric models. The facet joint space was simulated to be 0.5 mm [9]. A 0.2-mm-thick articular cartilage layer was added to both the superior and the inferior articular process, respectively [9]. To simplify the models and focus our analysis, we assumed that the articular surfaces of the C5/6 facet joints were planar.

The bone structure was then imported into Geomagic studio 15.0 (3D System Corporation, Rock Hill, South Carolina, USA) for model refinement by subdivision, noise reduction, smoothing, and surface fitting. The model was then constructed in Pro/E5.0 (Parametric Technology Corporation, Massachusetts, USA). By extending the inferior and superior endplates of the adjacent vertebrae, the intervertebral disc entities, including the cartilaginous endplate, nucleus pulposus,

and annulus fibrosus, were formed. The nucleus pulposus accounted for 44% of the disc space, and the annulus material accounted for 56% [19]. Within the annulus material, eight layers of annular fibers were arranged in opposite directions at 30° to 45° [19]. For each facet joint, cartilage and joint capsule were simulated. Finally, the anterior longitudinal ligament, posterior longitudinal ligament, ligamentum flavum, capsular ligament, intertransverse ligament, interspinous ligament and supraspinous ligament were added. The elastic modulus, Poisson's ratio, cross-sectional area and element type are shown in Table 1 [20–23].

Simulation of ACDR

The Prestige LP (Medtronic, Minnesota, USA), the Prodisc-C vivo (Johnson & Johnson, New Jersey, USA) and the Mobi-C (Zimmer Biomet, Indiana, USA) were simulated in this study. The three artificial intervertebral discs were scanned using laser scanning technology to obtain point clouds from physical products. The data obtained were then used to create three-dimensional models in PRO/E and Geomagic. After completing the modeling of the implants, they were assembled with the established spinal model in three dimensions. The height of all implants was set to 6 mm. The ACDR was simulated by inserting the artificial disc into the disc space after removal of the anterior longitudinal ligament, the intervertebral disc, and the posterior longitudinal ligament at the C5/C6 level. Three prostheses in the symmetrical model, the moderate asymmetrical model, and the severe asymmetrical model were made, making 9 models altogether. In all implant models, the position of the implant remains consistent, all implants were placed centrally in the coronal plane, maintaining consistency in the sagittal plane, and ensuring that the anterior and posterior edges of the implants did not extend beyond the vertebral margins. Among models featuring the same type of implant, the only variation lies in the tropism of the facet joints. The Prestige LP artificial disc material was assigned as titanium alloy (Ti6Al4V). The Prodisc-C Vivo and the Mobi-C were assigned as titanium alloy (Ti6Al4V) endplates and ultra-high molecular weight polyethylene (UHMWPE) core. Figure 1 includes a coronal view of the spine implanted with all cervical artificial discs.

Table 1 Material properties and mesh types of the cervical finite element model

	Modulus of elasticity(MPa)	Poisson ratio	Cross-sectional area (mm^2)	Element type
Cortical bone	12,000	0.30	/	C3D4
Trabecular bone	100	0.20	/	C3D4
Pedicles	3500	0.25	/	C3D4
Facet joint cartilage	15	0.45		C3D8
Cartilage endplate	24	0.25	/	C3D8
Nucleus pulposus	1	0.50	/	C3D8
Annulus fibrosus	4.2	0.45	/	C3D8
Annulus fibrosus fibers	175	/	0.76	T3D2
ALL	7.8	/	63.70	T3D2
PLL	1	/	20	T3D2
LF	1.5	/	40	T3D2
CL	7.5	/	30	T3D2
ITL	10	/	1.80	T3D2
IL	1	/	40	T3D2
SL	3	/	30	T3D2
Titanium alloy	110,000	0.3	/	/
PEEK	3660	0.3	/	/

ALL, anterior longitudinal ligament. PLL, posterior longitudinal ligament. LF, ligamentum flavum. CL, capsular ligament. ITL, intertransverse ligament. IL, interspinous ligament. SL, supraspinous ligament. PEEK, poly(ether-ether-ketone)

Boundary and loading condition

ABAQUS6.13 (SIMULIA, Rhode Island, US) was used to run the finite element models. A convergence analysis was performed on the intact model using the following method: The model underwent an initial meshing (The initial mesh size was set to be 1 ~ 2 mm), and extracted the nodes with the maximum stress in each model. Subsequently, the model's mesh was refined by a factor of two, and stress values from the same nodes were extracted. This process was iteratively repeated, doubling the mesh refinement until stress values converged. The mesh types for each component are as follows: The intervertebral disc, including the endplate, nucleus pulposus, and annulus fibrosus, are meshed using hexahedral elements. Ligaments and annulus fibrosus fibers are modeled using truss elements that only bear tensile loads. The vertebral bodies and implants are meshed using tetrahedral elements. The connections between vertebrae and intervertebral discs, vertebrae and facet cartilages, and ligament insertions to bones were designated as tie. The connection between the facet cartilages was simulated as a sliding contact without friction. The connection between reference point and vertebrae was designated as coupling. The upper and lower portions of the implants are attached to their respective vertebral bodies by fixed contact, simulating complete osseointegration of the implant with the bone and not allowing relative motion between the implants and the vertebral endplates. The contact between the portions of the implants was modeled as a surface-to-surface contact definition, surface friction coefficients were set at 0.1 between the two metal plates for the Prestige LP prosthesis and 0.3 between the metal and polymer surfaces for the Prodisc C vivo, and Mobi-C prostheses [18]. The cervical model was fixed with six degrees of freedom at the inferior endplate of the T1 vertebra. A 75 N follower loading was used to represent the head's weight [9, 24]. In addition to the follower load, a 1.0 Nm moment was applied to the C2 vertebrae

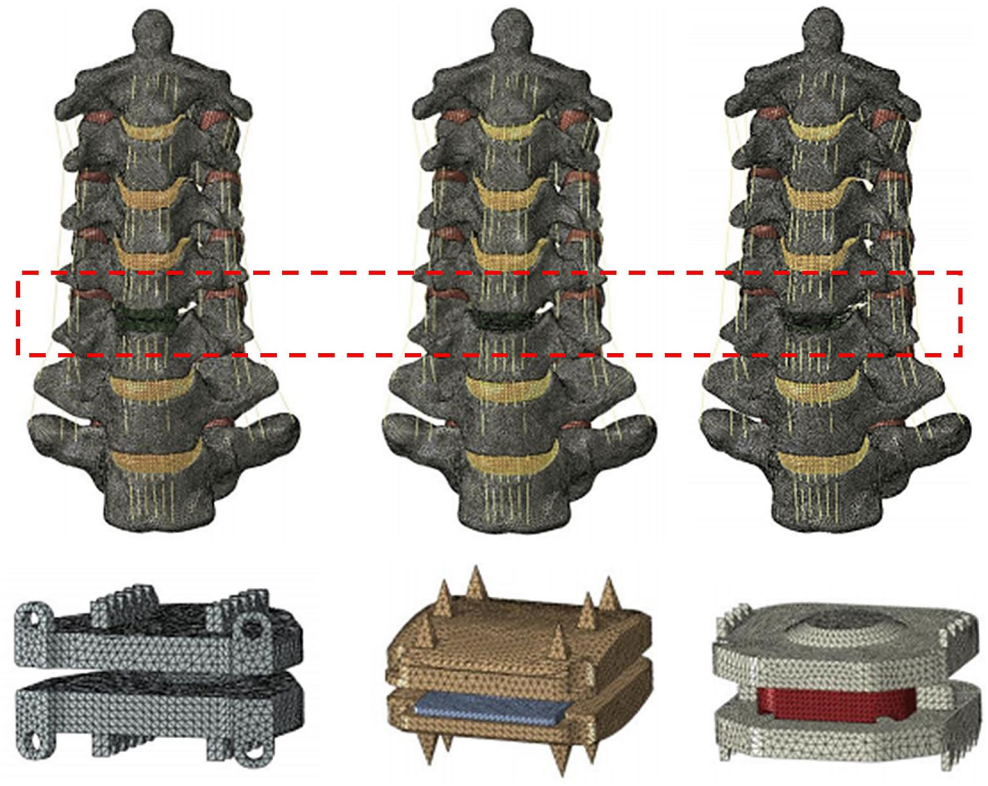

Fig. 1 Coronal views from left to right of Prestige LP, Prodisc C vivo, and Mobi-C and spine models. Dashed rectangle shows the level of cervical disk arthroplasties, i.e., at the C5–C6 level

to produce flexion, extension, lateral bending, and axial rotation [9, 24]. The range of motions (ROMs) under all moments, as well as FCFs and facet capsule stress were tested. FCFs and facet capsule stress were not measured directly; instead, they were computed through post-processing in Abaqus. Contact forces and capsular tension were extracted, and stress was calculated using the formula stress=force/area.

Result

Validation of the symmetrical model

The ROM of each motion segment in the symmetrical intact model under 1.0 Nm moments is presented in Fig. (2). The ROM values of the symmetrical intact model fell within the range of ROMs previously reported in literature [25–27].

The C5/C6 ROMs

The segmental C5-C6 ROMs after C5/C6 arthroplasty using different devices are shown in Fig. (3). It indicates increased flexion-extension, lateral bending, and rotation in symmetric, moderate asymmetric, and severe asymmetric models. The largest increase in flexion-extension ROM occurred after simulating Prodisc-C Vivo in the severe asymmetric model. Similarly, the largest increase in lateral bending ROM was observed after simulating Prestige-LP, while the largest increase in rotation ROM was noted after simulating Mobi-C. Notably, in the moderate asymmetric model, the flexion-extension ROM decreased after simulating Mobi-C, while the rotation ROM decreased after simulating Prestige-LP and Mobi-C, as compared to the symmetric model.

Facet contact forces

Under 75 N preload, the left-sided and right-sided FCFs of different models in different states are shown in the histograms. All three implants resulted in increased FCFs on both sides in extension, lateral bending, and rotation, compared to the intact model (Fig. 4). Under asymmetric conditions, the difference in FCFs between the implant models and the intact model is generally larger than under symmetric conditions in the majority of positions (Figs. 5 and 6).

Under moderate asymmetric conditions, the left-side FCFs of all models decreases in neutral, extension, left bending, and right rotation compared to symmetric conditions. During extension, the left-side FCFs of Prestige-LP, Prodisc-C, and Mobi-C models are only 7.4%, 2.3%, and 4.4% of those under symmetric conditions, respectively. Under left rotation, the left-side FCFs of all models increases compared to symmetric conditions. With an increase in asymmetry, different changes were observed.

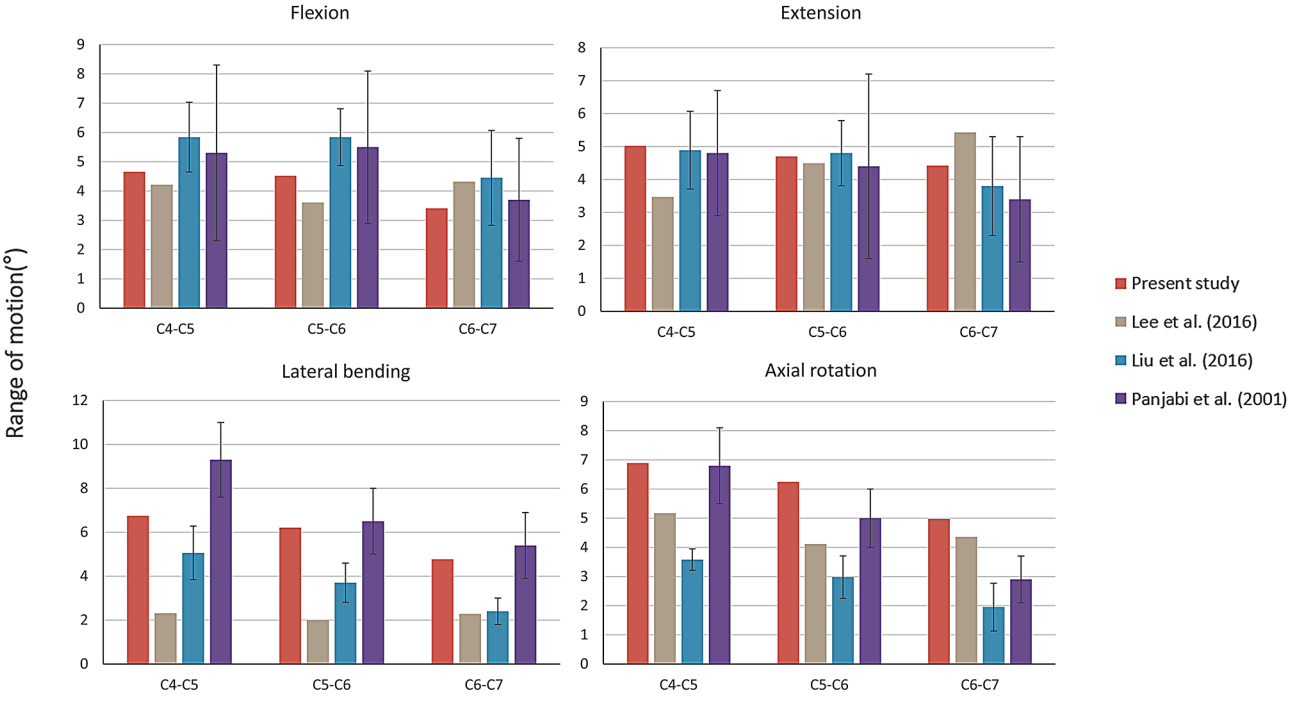

Fig. 2 Comparison of the predicted range of motion of current symmetrical intact model and previous reported data

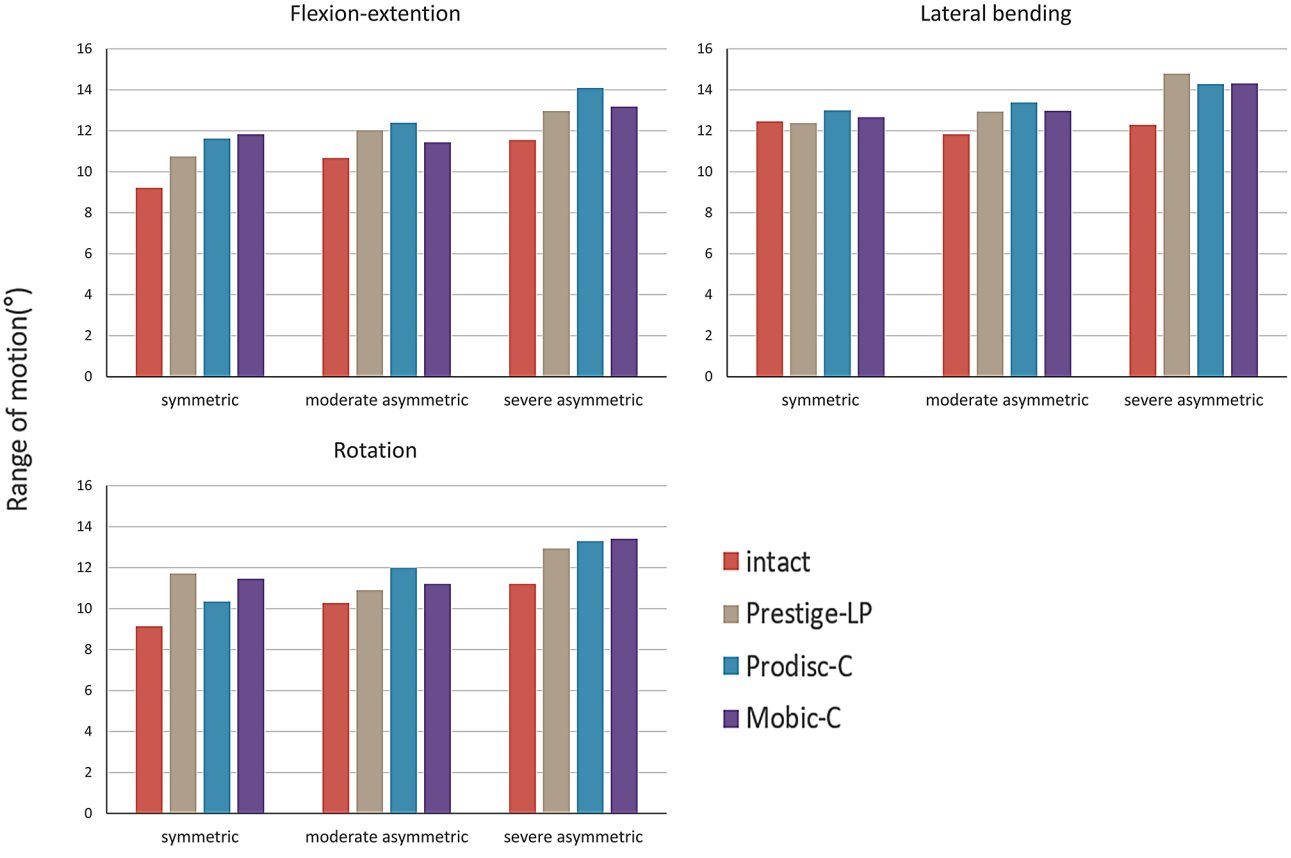

Fig. 3 Range of motions (ROM) at C5/C6 level in the symmetrical model, the moderate asymmetrical model, and the severe asymmetrical model before and after simulated ACDR with different implants in different motion

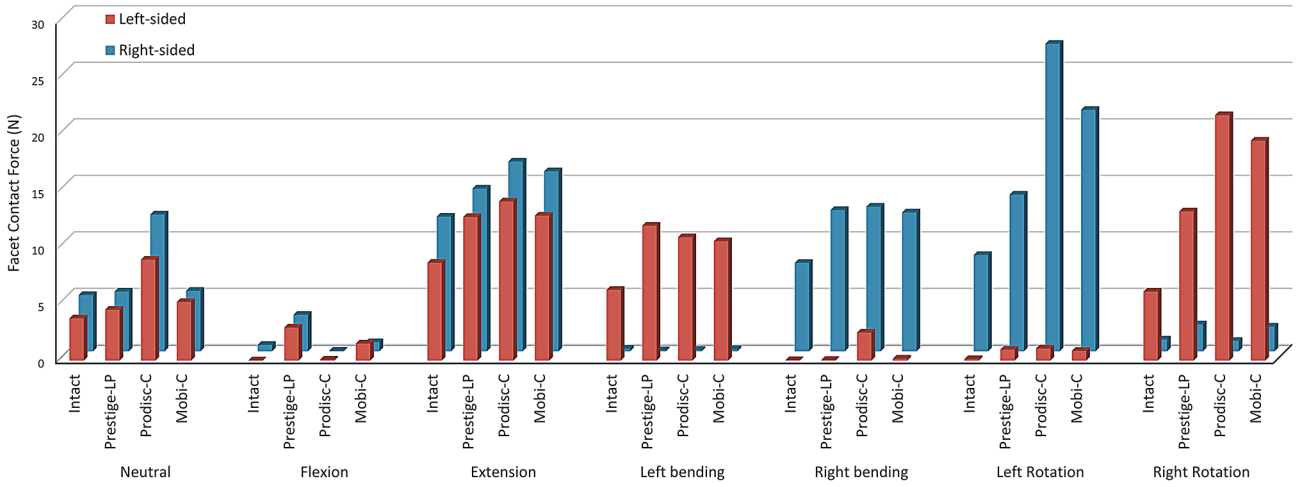

Fig. 4 Facet contact forces (FCFs) at the C5/C6 level in the symmetrical model before and after simulated ACDR with different implants in neutral position under 75 N preload and different motion condition under 1 N·m moment plus 75 N follower load

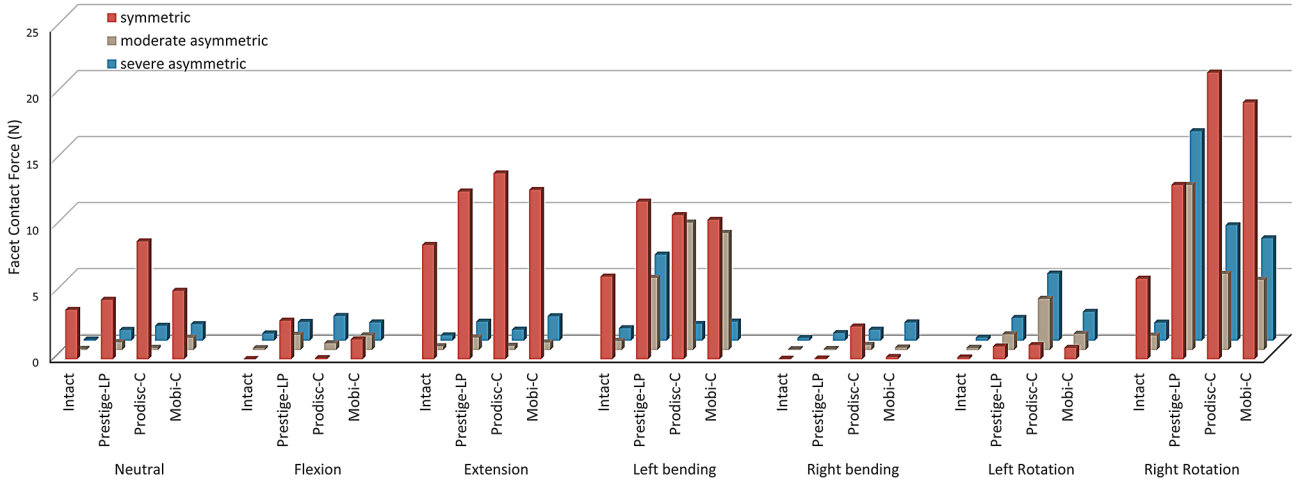

Fig. 5 Left side Facet contact forces (FCFs) at the C5/C6 level in the symmetrical model, the moderate asymmetrical model, and the severe asymmetrical model before and after simulated ACDR with different implants in neutral position under 75 N preload and different motion condition under 1 N·m moment plus 75 N follower load

Under severe asymmetric conditions, in most positions, the left-side FCFs of all models increases compared to mild asymmetric conditions, except for the Prodisc-C and Mobi-C models, where the left facet stress further decreases during left bending. During left rotation, the left-side FCFs of Prestige-LP, Prodisc-C, and Mobi-C models are 1.79 times, 4.79 times, and 2.56 times higher, respectively, under severe asymmetric conditions compared to symmetric conditions (Fig. 5).

The pattern of right-side FCFs differs from the left side. In neutral, extension, right bending, and left rotation, all models show a gradient increase in right-side FCFs under symmetric, moderate asymmetric, and severe asymmetric conditions. During right bending under severe asymmetric conditions, the right facet contact forces of Prestige-LP, Prodisc-C, and Mobi-C models are 3.14 times, 3.11 times, and 2.61 times higher, respectively, compared to symmetric conditions (Fig. 6).

Facet stress distribution

The stress distribution on the left and right-side facet in the symmetrical model demonstrated negligible differences in neutral, flexion, and extension positions. And the stress distribution on left and right-side facet is opposite in the position of left and right bending. Conversely, in the asymmetric model, the stress distribution displayed a distinct pattern. High stress was observed on the anterior portion of the left facet joint in all asymmetric models (supplementary materials), During left bending and right rotation, The stress on the right facet joint is also distributed more towards the cranial side, opposite to the symmetric condition (Figs. 7 and 8).

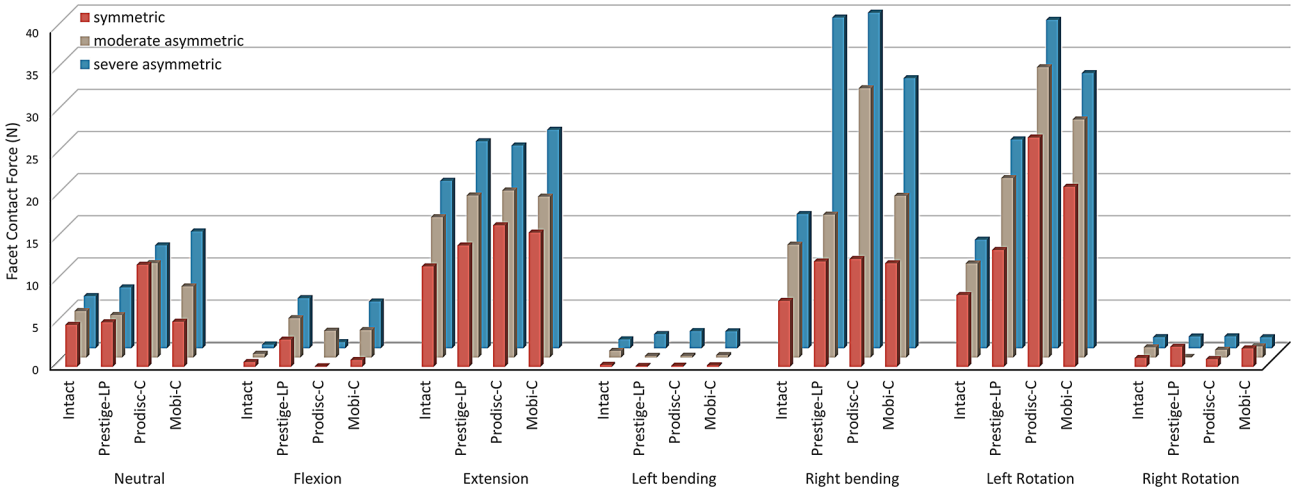

Fig. 6 Right side Facet contact forces (FCFs) at the C5/C6 level in the symmetrical model, the moderate asymmetrical model, and the severe asymmetrical model before and after simulated ACDR with different implants in neutral position under 75 N preload and different motion condition under 1 N·m moment plus 75 N follower load

Left bending

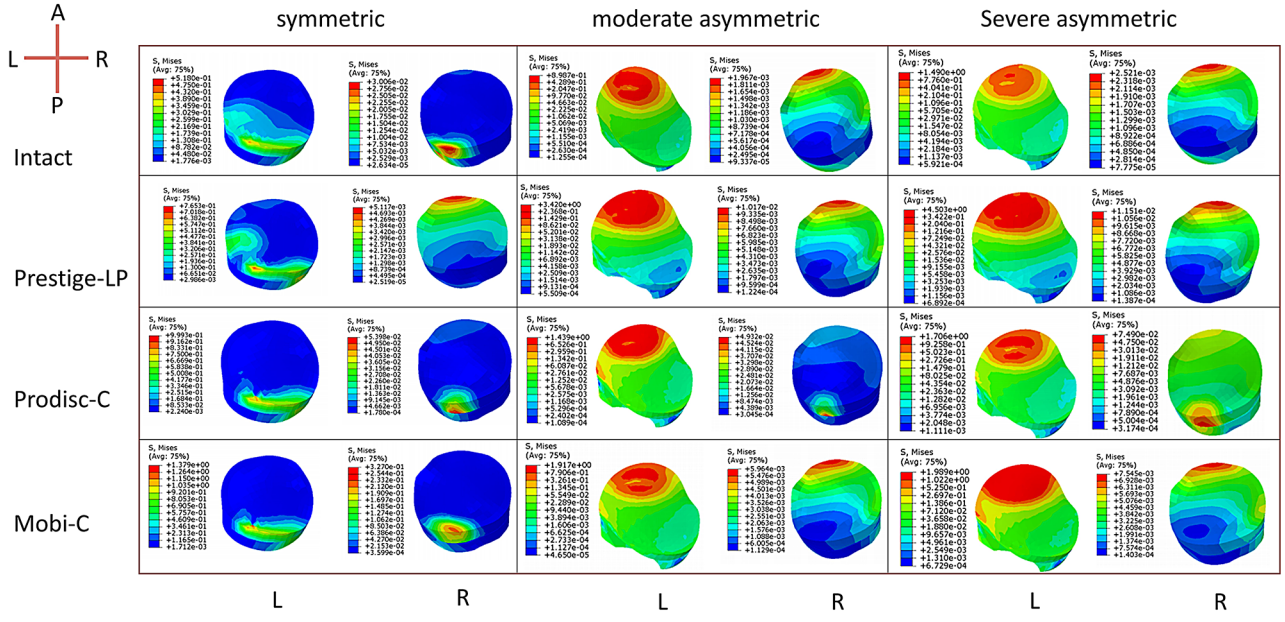

Fig. 7 Stress distribution on the joint surfaces of the C6 superior articular process before and after simulated C5/C6 ACDR with different implants in the symmetrical model, the moderate asymmetrical model, and the severe asymmetrical model in left bending under 1 N·m moment plus 75 N follower load. (L, left side. R, right side. C, anterior portion. P, posterior portion)

Facet capsule stress

In the symmetric model, the stress on the facet capsule on both the left and right sides showed similar values in neutral, flexion, and extension positions both before and after simulating ACDR with different implants. However, during left or right bending or rotation, the facet capsule stress on the left side was greater while that on the right side was smaller, and vice versa. Notably, the facet capsule stress increased in all positions after simulating all three implants compared to the intact model, with a more significant increase observed in the asymmetrical model. The study found that the Mobi-C implant had the highest impact on capsule stress when severe facet tropism was present, with the facet capsule stress on the left and right sides increasing by 14 times and 3.7 times, respectively, under right rotation compared to the symmetric model. Interestingly, the Prodisc-C implant showed the lowest bilateral facet capsule stress in the extended position in the symmetric model but had the highest in the asymmetric model, as shown in (Figs. 9, 10 and 11).

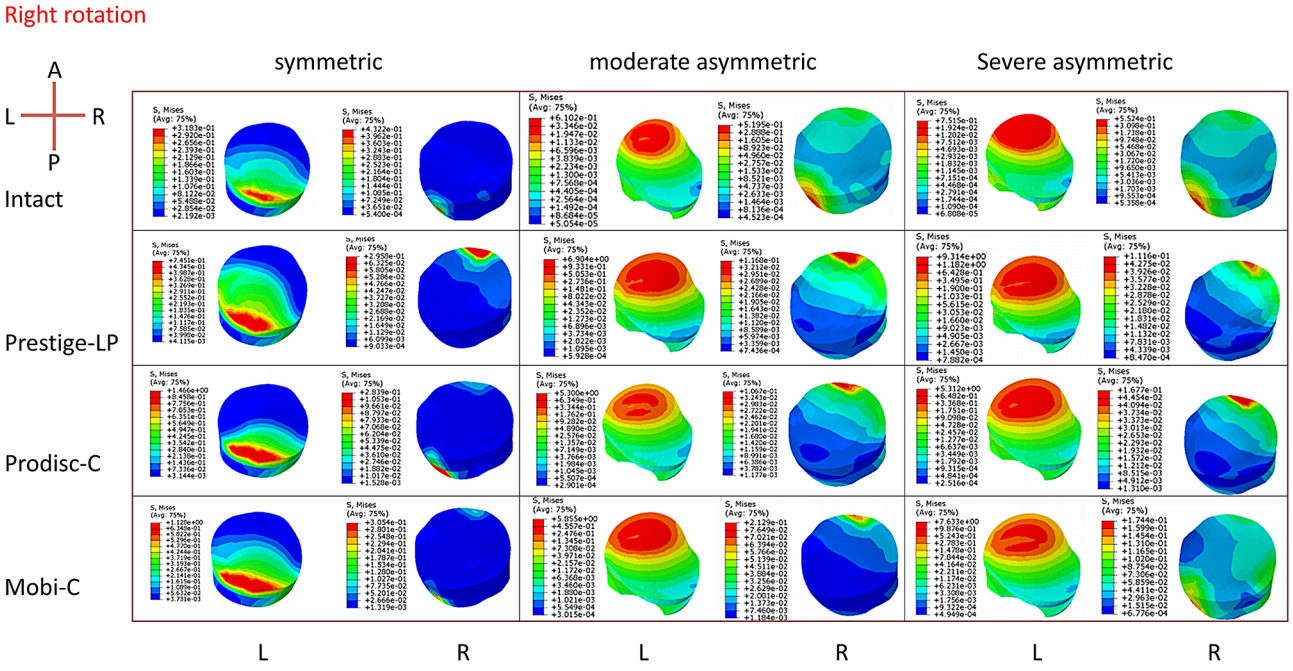

Fig. 8 Stress distribution on the joint surfaces of the C6 superior articular process before and after simulated C5/C6 ACDR with different implants in the symmetrical model, the moderate asymmetrical model, and the severe asymmetrical model in right rotation under 1 N·m moment plus 75 N follower load. (L, left side. R, right side. C, anterior portion. P, posterior portion)

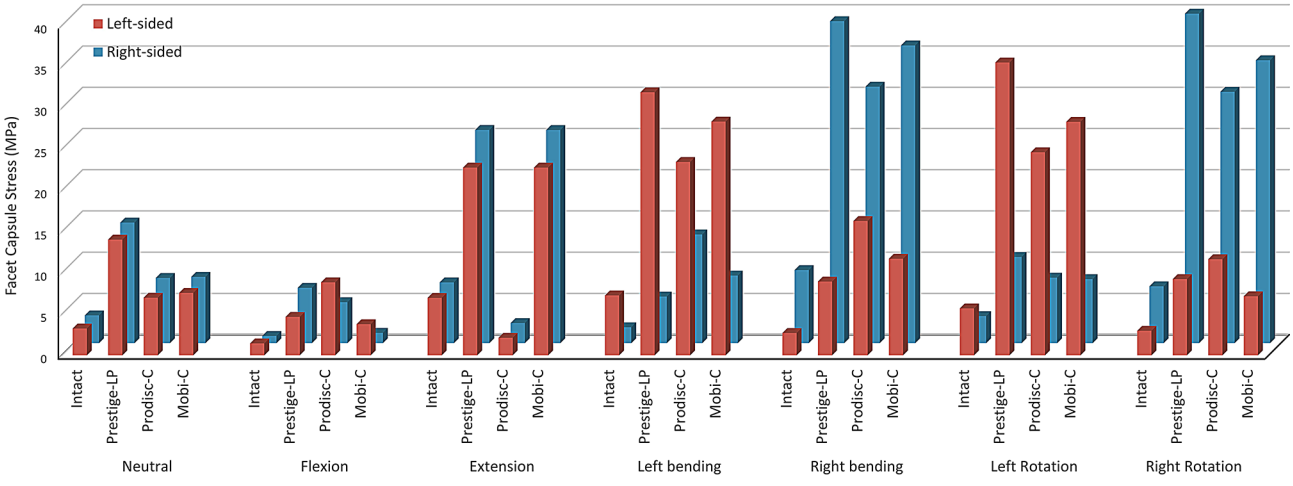

Fig. 9 Facet capsule stress at the C5/C6 level in the symmetrical model before and after simulated ACDR with different implants in neutral position under 75 N preload and different motion condition under 1 N·m moment plus 75 N follower load

In neutral, flexion, and extension, the facet capsule stress of all models is evenly distributed on both sides of the bilateral facets. During lateral bending, the stress is concentrated on the flexion side of the ipsilateral facet and the extension side of the contralateral facet. Under these conditions, the stress distribution patterns of the asymmetric and symmetric models are similar, with no significant differences observed (supplementary materials). During left rotation, under asymmetric conditions, the right facet capsule stress of the intact, Prestige-LP, and Mobi-C models is concentrated posteriorly, differing from the symmetric condition. Conversely, in the Prodisc-C model, under asymmetric conditions, no concentrated stress was observed, while under symmetric conditions, the right facet capsule stress is concentrated posteriorly (Fig. 12). During right rotation under symmetric conditions, the left facet capsule stress of the complete and Prestige-LP models is concentrated to the right posterior, while in the Prodisc-C and Mobi-C models, it is concentrated to the left posterior. Under asymmetric conditions, no concentrated stress was observed. During right rotation, no significant differences were observed in

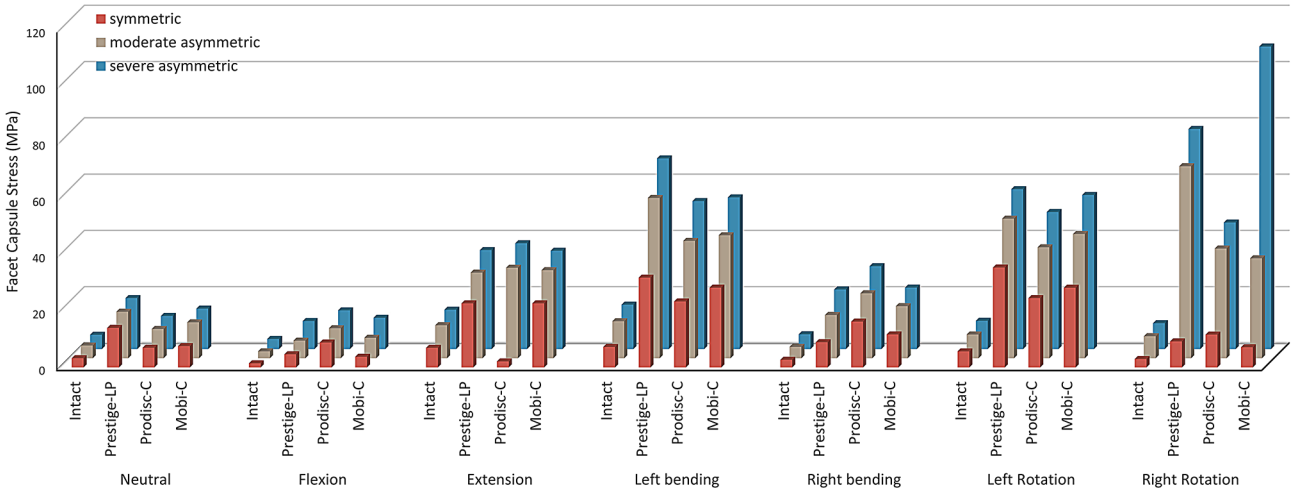

Fig. 10 Left side facet capsule stress at the C5/C6 level in the symmetrical model, the moderate asymmetrical model, and the severe asymmetrical model before and after simulated ACDR with different implants in neutral position under 75 N preload and different motion condition under 1 N·m moment plus 75 N follower load

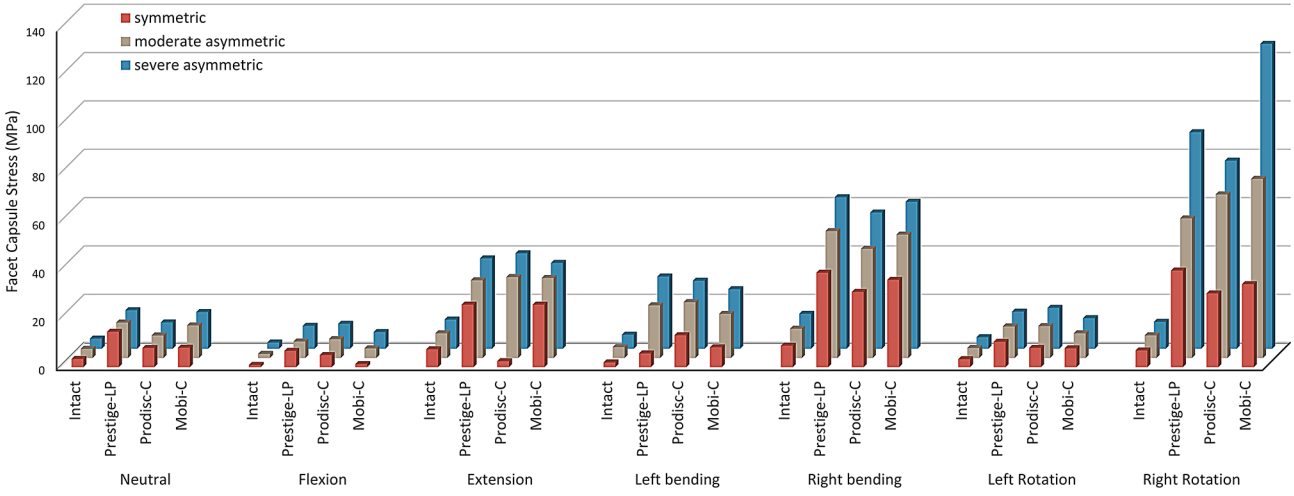

Fig. 11 Right side facet capsule stress at the C5/C6 level in the symmetrical model, the moderate asymmetrical model, and the severe asymmetrical model before and after simulated ACDR with different implants in neutral position under 75 N preload and different motion condition under 1 N·m moment plus 75 N follower load

the distribution of capsule stress on the right side under symmetric and asymmetric conditions (Fig. 13).

Discussion

The intervertebral discs and facet joints are integral components of the spinal column and their complex interplay can exert a significant influence on each other. Facet tropism, an asymmetry between paired facet joint orientations, has been implicated in lumbar spine degeneration. Specifically, Kong et al. [28] demonstrated that lumbar facet tropism leads to severe degeneration of the facet joints at the L4/L5 level. Our previous investigation [29] corroborated the relationship between facet tropism and facet degeneration in the cervical spine. Additionally, several studies have reported a correlation between facet tropism and intervertebral disc herniation [30–32]. In a recent finite element analysis, we examined the impact of facet tropism on intervertebral disc pressure and facet contact forces (FCFs) during different movements [9]. Our findings indicate that facet tropism significantly increases the FCFs and intervertebral disc pressure at the index level, suggesting that abnormal stress resulting from facet tropism may contribute to cervical spine degeneration. Previous studies have shown that ACDR may lead to abnormal stress on the facet joints, potentially accelerate the facet degeneration process. Our current study demonstrated that facet tropism further exacerbated the force exerted on facet joints after ACDR. The extent of this exacerbation was found to be influenced by the type of prosthesis design employed.

Left rotation

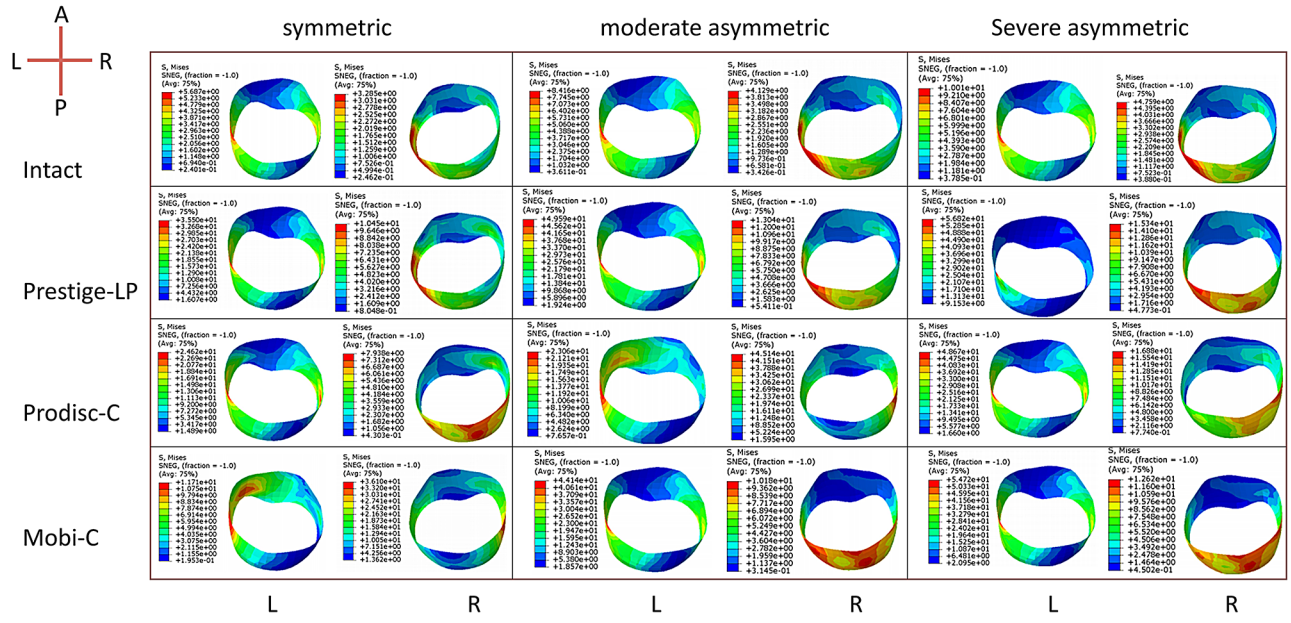

Fig. 12 The C5/C6 Facet capsule stress distribution before and after simulated C5/C6 ACDR with different implants in the symmetrical model, the moderate asymmetrical model, and the severe asymmetrical model in left rotation under 1 N·m moment plus 75 N follower load. (L, left side. R, right side. C, anterior portion. P, posterior portion)

Right rotation

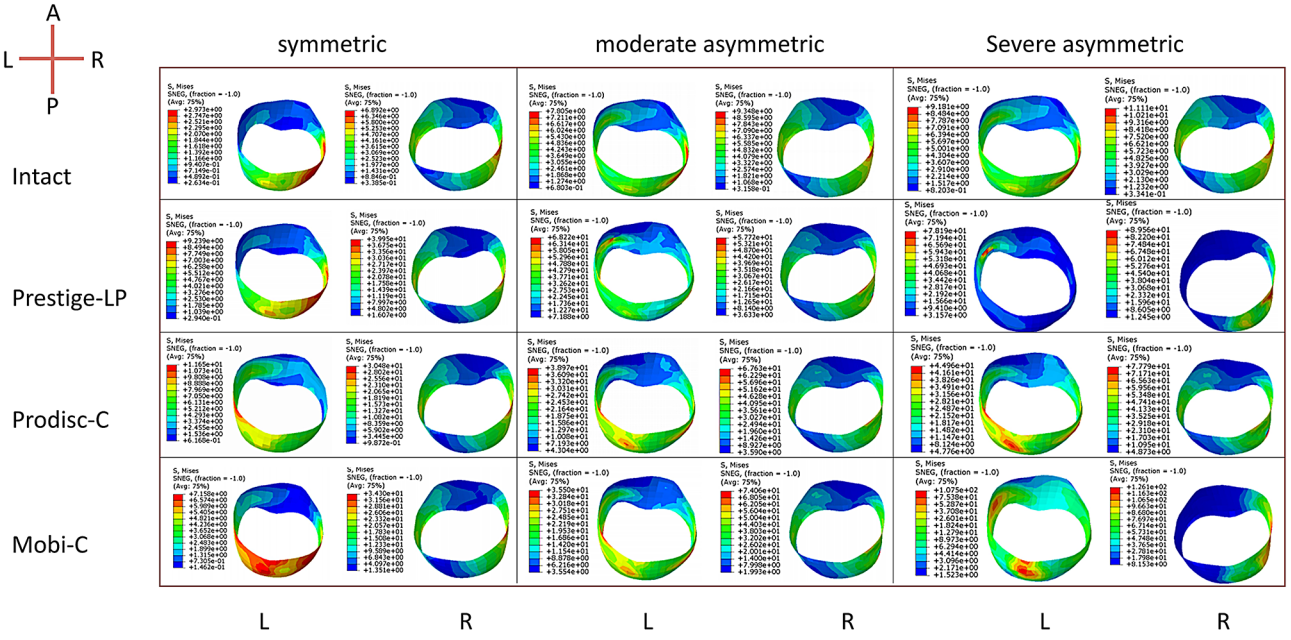

Fig. 13 The C5/C6 Facet capsule stress distribution before and after simulated C5/C6 ACDR with different implants in the symmetrical model, the moderate asymmetrical model, and the severe asymmetrical model in right rotation under 1 N·m moment plus 75 N follower load. (L, left side. R, right side. C, anterior portion. P, posterior portion)

We observed that in the presence of facet tropism, all ACDR models exhibited significantly higher FCFs and facet capsule stress compared to the intact model, especially during flexion, extension, rotation, and lateral bending. We speculate that the underlying reason for these outcomes may be related to the altered relative motion of the facet joint surfaces in the presence of facet tropism during cervical spine motion. Taking rotational

movement as an example, during axial rotation, the upper and lower facet joint surfaces undergo relative sliding in the horizontal direction. However, due to the inclination of the facet joint surfaces relative to the horizontal plane, the two surfaces overlap on the side where rotation occurs and separate on the opposite side during the sliding process [33]. In this process, the two joint surfaces inevitably experience compression, and the asymmetry of the facet joints exacerbates the bilateral joint motion imbalance, resulting in an abnormal increase in FCFs. Simultaneously, this abnormal relative motion may lead to changes in the relative positions of the joint surfaces during the end of the motion, subsequently causing abnormal stretching of the joint capsule, resulting in increased facet capsule stress. This aligns with the abnormal distribution of joint surface and capsular stresses observed in our test results during lateral bending and axial rotation. This phenomenon was also observed in the intact model, but in the ACDR models, the implants acted as amplifiers, significantly increasing the magnitude of these effects, this may be due to the surgical removal of the intervertebral discs and posterior longitudinal ligaments, which are important structures for maintaining the stability of the cervical spine during motion [13, 14], resulting in greater reliance on the posterior column structures to maintain stability during motion, which in turn leads to higher FCFs and facet capsule stresses.

The design of the prosthesis used in surgery including core material, core mobility, center of prosthetic motion, etc., may have different effects on the biomechanical environment of the facet joints [18, 34–40]. The Prestige-LP is a two-piece metal-on-metal device that is semi-constrained, allowing for 2 mm of forward and backward movement, and over 10° of flexion, extension, and lateral bending. Due to its rigid metal-to-metal structure, load transmitting in the anterior and middle column is facilitated, resulting in lower FCFs than Prodisc-C Vivo and Mobi-C in the symmetrical model. This effect is similar to the stress shielding phenomenon. Lin CY et al. [35] have also compared the Prestige-LP, Prodisc-C, and Bryan intervertebral discs and found that the Prestige-LP had significantly lower segmental displacement than the Prodisc-C under compression and lateral bending conditions. They concluded that a rigid core can better distribute the load and reduce the load on the facet joints. Similar conclusions were drawn by Kang H et al. [37] who suggested that the stiffness of the core material plays a major role in load sharing when comparing artificial intervertebral discs. However, this advantage is lost in the asymmetric model, where the asymmetry of the facet joints leads to a stress concentration on one of the facet joint surfaces, partially alleviating the load transmitted through the metal-to-metal interface. This effect becomes more pronounced with increasing asymmetry, as evidenced by the maximum difference in FCF observed between the moderate and severe asymmetric models. In addition, the change in moment arm length due to a moving centre of rotation should be considered. Choi et al. [8] found that the FCF increased by 13.0% and 183.9% for the Bryan disc and Prodisc-C respectively under extension. This may be due to the change in moment arm length caused by the moving centre of rotation of the Bryan prosthesis.

The Prodisc-C Vivo and Mobi-C artificial discs are similar in construction, consisting of cobalt chromium endplates and polyethylene components. However, the Prodisc-C Vivo is a semi-constrained device with a fixed centre of rotation, whereas the Mobi-C is an un constrained device with a mobile core and no fixed centre of rotation. Our results showed that the FCFs of both devices were similar in symmetrical models. However, in the asymmetric model, the Mobi-C model had lower FCFs than the Prodisc-C Vivo, but the facet capsule stresses were instead higher. This finding may be due to the greater adaptability of the nonfixed core of Mobi-C, which enables the coupling of the facet joints to adapt to the patient's anatomy resulting in lower FCFs in the presence of facet tropism, but this also results in a change in the relative position of the upper and lower articular surfaces at the end of the movement, leading to higher facet capsule stresses. This finding is in contrast to the previous conclusion by Kang et al. [37] that a constrained implant could potentially exacerbate instability and lead to joint protrusion over time. We speculate that differences in patient anatomy and facet tropism may make it difficult for a fixed core to fit each individual, particularly in the presence of facet joint asymmetry. Therefore, a non-fixed core, as in the case of Mobi-C, may offer greater adaptability. However, this adaptability may also result in the core being off-centre from the vertebral body, leading to a concentration of forces on one side of the vertebral body. It is unclear whether this may cause long-term problems or exacerbate instability when the degree of asymmetry exceeds the adjustable range. Further research is needed to clarify these issues.

In terms of mobility, the surgical segment mobility of all implant models was found to be greater than that of the intact model in all cases. This indicates that the range of motion is preserved with the implant, but the pattern of motion (such as the center of rotation) may change. We found that the differences in segment mobility among the three intervertebral discs were within 2° in different models, which is not clinically significant. However, there was a trend of increased mobility in asymmetric conditions. Although the magnitude of the increase was not significant, we found that the slight increase in mobility of the anterior column resulted in significant changes in

the stress of the posterior facet joint capsule. The biomechanical changes caused by the increase in ROM in the surgical segment are visually reflected in changes in facet capsule stress. In the comparison of each model, the maximum ROM in each direction and the maximum facet capsule stress during motion in that direction showed a one-to-one correspondence. In the severe asymmetric model, the Prodisc-C model had the greatest flexion-extension ROM, and the largest observed facet capsule stress during flexion-extension was also seen in the Prodisc-C model. The same phenomenon occurred in the Prestige-LP model during lateral bending and the Mobi-C model during rotation. While it is understandable that greater mobility would result in greater stress on the facet joints, it is worth noting that the actual results seem to contradict the theory that non- constrained core implants would provide greater mobility. The Prestige-LP, which has the greatest core mobility in the anterior-posterior direction, actually had the lowest flexion-extension mobility of the three implants, while the non- constrained core Mobi-C also exhibited lower mobility in most cases. This phenomenon may be explained by the fact that a mobile core allows for better coupling of the upper and lower joint surfaces of the posterior facet joint through its movement, resulting in greater stability.

There are several limitations to this study. In terms of model establishment, firstly, the cervical spine model used in this study was based on a young male with no symptoms and assumed the facet surface them as planar. Other finite element studies have shown that degenerative factors of the cervical spine, such as intervertebral space height, disc degeneration, facet joint distance and facet joint degeneration, can alter the mechanical environment of the posterior column [41–44]. Secondly, the establishment of the intervertebral disc model in this study is relatively straightforward. Other disc models, including poroelastic models, have been proposed in previous research to simulate the biomechanical changes resulting from various pathophysiological conditions of the intervertebral disc [45]. Thirdly, bone density may have an impact on postoperative biomechanics; studies have found uneven distribution of cervical spine bone density [46], which could influence the results differently. Additionally, changes in vertebral composition and morphological characteristics can also lead to variations in mechanical properties. Previous studies have found that linear combinations of bone volume fraction, trabecular thickness, trabecular spacing, structure model index, connectivity density, and degree of anisotropy provide a correlation with aggregate modulus [47]. Incorporating all these factors into the FE model construction would undoubtedly enhance the model's effectiveness, allowing it to closely approximate the real cervical spine structure. However, due to the inherent limitations of FE analysis, it remains challenging to include all factors, such as the influence of muscles on the cervical spine. Therefore, creating such a complex model may seem of limited significance. In this study, FE serves as a tool for judging the trends in the results rather than obtaining precise numerical data. The trends obtained through FE can effectively guide clinicians to pay more attention to the impact of facet tropism, inspiring further research. Integrating the mentioned factors into future studies may lead to more intriguing discoveries. Furthermore, the three artificial prostheses evaluated in this study were all ball-and-socket prostheses. Other prostheses with different structures, such as the non-ball and socket Bryan prosthesis, the M6-C leaf spring prosthesis, the Discover cog prosthesis, the multilevel segmented Simplify prosthesis, and the PCM plate prosthesis, may have a different effect on the cervical spine in the presence of facet tropism.

Conclusions

The existence of facet tropism could considerably increase FCFs and facet capsule stress after ACDR. In the presence of facet tropism, none of the three artificial discs, Prestige-LP, Prodisc-C Vivo, and Mobi-C, protected the facet joints; in patients with facet tropism, new artificial discs may need to be developed to deal with this situation. Clinical trials are needed to validate the impact of facet tropism.

Supplementary Information

The online version contains supplementary material available at https://doi.org/10.1186/s13018-024-05218-5.

Supplementary Material 1

Author contributions

JL and YL wrote the main manuscript text. JL, YL and JQZ made substantial contribution to analysis and interpretation of data. HL, RX, BYW, and KKH made substantial contributions to conception and design. XR gave the final approval of the version to be published. All authors read and approved the final manuscript.

Funding

This study was supported by the Sichuan Provincial Department of Science and Technology Applied Basic Research (2022NSFSC0595) for analysis and interpretation of data.

Data availability

The raw data supporting the conclusion of this article will be made available by the authors, without undue reservation.

Declarations

Ethical approval

This study was approved by the Ethical Committee of West China Hospital of Sichuan University. All patients had given the informed consent to allow their information to be used in research purposes.

Competing interests

The authors declare no competing interests.

Author details
[1]Department of Orthopedics, Orthopedic Research Institute, West China Hospital, Sichuan University, Chengdu, China
[2]Department of Orthopedics Surgery, West China Hospital, Sichuan University/West China School of Nursing, Sichuan University, Chengdu, China

Received: 31 October 2023 / Accepted: 26 October 2024
Published online: 30 October 2024

References

1. Loidolt T, Kurra S, Riew KD, et al. Comparison of adverse events between cervical disc arthroplasty and anterior cervical discectomy and fusion: a 10-year follow-up. Spine J. 2021;21:253–64.
2. Lavelle WF, Riew KD, Levi AD, et al. Ten-year Outcomes of Cervical Disc Replacement With the BRYAN Cervical Disc: Results From a Prospective, Randomized, Controlled Clinical Trial. Spine (Phila Pa 1976). 2019;44:601–8.
3. Gornet MF, Lanman TH, Burkus JK et al. 2019. Two-level cervical disc arthroplasty versus anterior cervical discectomy and fusion: 10-year outcomes of a prospective, randomized investigational device exemption clinical trial. J Neurosurg Spine. 2019 Jun 21;31(4):508-518.
4. Gornet MF, Burkus JK, Shaffrey ME, et al. Cervical disc arthroplasty: 10-year outcomes of the Prestige LP cervical disc at a single level. J Neurosurg Spine. 2019;31:317–25.
5. Peng Z, Hong Y, Meng Y, et al. A meta-analysis comparing the short- and mid- to long-term outcomes of artificial cervical disc replacement(ACDR) with anterior cervical discectomy and fusion (ACDF) for the treatment of cervical degenerative disc disease. Int Orthop. 2022;46:1609–25.
6. Wagner SC, Formby PM, Kang DG, et al. Persistent axial neck pain after cervical disc arthroplasty: a radiographic analysis. Spine J. 2016;16:851–6.
7. Purushothaman Y, Yoganandan N, Jebaseelan D, et al. External and internal responses of cervical disc arthroplasty and anterior cervical discectomy and fusion: A finite element modeling study. J Mech Behav Biomed Mater. 2020;106:103735.
8. Choi H, Purushothaman Y, Baisden JL, et al. Comparative Finite Element Modeling Study of Anterior Cervical Arthrodesis Versus Cervical Arthroplasty With Bryan Disc or Prodisc C. Mil Med. 2021;186:737–44.
9. Rong X, Wang B, Ding C, et al. The biomechanical impact of facet tropism on the intervertebral disc and facet joints in the cervical spine. Spine J. 2017;17:1926–31.
10. Cyron BM, Hutton WC. Articular tropism and stability of the lumbar spine. Spine (Phila Pa 1976). 1980;5:168–72.
11. Gallucci M, Puglielli E, Splendiani A, et al. Degenerative disorders of the spine. Eur Radiol. 2005;15:591–8.
12. Rong X, Liu Z, Wang B et al. 2017. The Facet Orientation of the Subaxial Cervical Spine and the Implications for Cervical Movements and Clinical Conditions. Spine (Phila Pa 1976) 42:E320-E325.
13. Yong-Hing K, Kirkaldy-Willis WH. The pathophysiology of degenerative disease of the lumbar spine. Orthop Clin North Am. 1983;14:491–504.
14. Kirkaldy-Willis WH, Farfan HF. 1982. Instability of the lumbar spine. Clin Orthop Relat Res. 1982 May;(165):110-23.
15. Palissery V, Mulholland RC, McNally DS. The implications of stress patterns in the vertebral body under axial support of an artificial implant. Med Eng Phys. 2009;31:833–7.
16. Ganbat D, Kim YH, Kim K, et al. Effect of mechanical loading on heterotopic ossification in cervical total disc replacement: a three-dimensional finite element analysis. Biomech Model Mechanobiol. 2016;15:1191–9.
17. Khalaf K, Nikkhoo M. Comparative biomechanical analyses of lower cervical spine post anterior fusion versus intervertebral disc arthroplasty: A geometrically patient-specific poroelastic finite element investigation. J Orthop Translat. 2022;36:33–43.
18. Purushothaman Y, Choi H, Yoganandan N, et al. A Comparison Study of Four Cervical Disk Arthroplasty Devices Using Finite Element Models. Asian Spine J. 2021;15:283–93.
19. Johnson EF, Chetty K, Moore IM, et al. The distribution and arrangement of elastic fibres in the intervertebral disc of the adult human. J Anat. 1982;135:301–9.
20. Fan W, Guo LX. The effect of non-fusion dynamic stabilization on biomechanical responses of the implanted lumbar spine during whole-body vibration. Comput Methods Programs Biomed. 2020;192:105441.
21. Hua W, Zhi J, Wang B, et al. Biomechanical evaluation of adjacent segment degeneration after one- or two-level anterior cervical discectomy and fusion versus cervical disc arthroplasty: A finite element analysis. Comput Methods Programs Biomed. 2020;189:105352.
22. Li XF, Lv ZD, Yin HL, et al. Impact of adjacent pre-existing disc degeneration status on its biomechanics after single-level anterior cervical interbody fusion. Comput Methods Programs Biomed. 2021;209:106355.
23. Wu TK, Meng Y, Liu H, et al. Biomechanical effects on the intermediate segment of noncontiguous hybrid surgery with cervical disc arthroplasty and anterior cervical discectomy and fusion: a finite element analysis. Spine J. 2019;19:1254–63.
24. Shen YW, Yang Y, Liu H, et al. Biomechanical Evaluation of Intervertebral Fusion Process After Anterior Cervical Discectomy and Fusion: A Finite Element Study. Front Bioeng Biotechnol. 2022;10:842382.
25. Lee JH, Park WM, Kim YH et al. 2016. A Biomechanical Analysis of an Artificial Disc With a Shock-absorbing Core Property by Using Whole-cervical Spine Finite Element Analysis. Spine (Phila Pa 1976) 41:E893-E901.
26. Liu Q, Guo Q, Yang J, et al. Subaxial Cervical Intradiscal Pressure and Segmental Kinematics Following Atlantoaxial Fixation in Different Angles. World Neurosurg. 2016;87:521–8.
27. Panjabi MM, Crisco JJ, Vasavada A, et al. Mechanical properties of the human cervical spine as shown by three-dimensional load-displacement curves. Spine (Phila Pa 1976). 2001;26:2692–700.
28. Kong MH, He W, Tsai YD, et al. Relationship of facet tropism with degeneration and stability of functional spinal unit. Yonsei Med J. 2009;50:624–9.
29. Rong X, Liu Z, Wang B, et al. Relationship between facet tropism and facet joint degeneration in the sub-axial cervical spine. BMC Musculoskelet Disord. 2017;18:86.
30. Zhou Y, Wang B, Pei Z, et al. Facet tropism: Association between cervical disc degeneration and cervical spondylotic radiculopathy in middle-aged patients. J Clin Neurosci. 2022;99:89–93.
31. Wang Y, Chen G, Lin J et al. 2021. The Correlation Between Facet Tropism and Intervertebral Disc Herniation in the Subaxial Cervical Spine. Spine (Phila Pa 1976) 46:E310-E317.
32. Huang X, Ye L, Liu X, et al. The relationship between facet tropism and cervical disc herniation. J Anat. 2020;236:916–22.
33. Bogduk N, Mercer S. Biomechanics of the cervical spine. I: Normal kinematics. Clin Biomech (Bristol Avon). 2000;15:633–48.
34. Rousseau MA, Bonnet X, Skalli W. Influence of the geometry of a ball-and-socket intervertebral prosthesis at the cervical spine: a finite element study. Spine (Phila Pa 1976). 2008;33:E10–14.
35. Lin CY, Kang H, Rouleau JP, et al. Stress analysis of the interface between cervical vertebrae end plates and the Bryan, Prestige LP, and ProDisc-C cervical disc prostheses: an in vivo image-based finite element study. Spine (Phila Pa 1976). 2009;34:1554–60.
36. Galbusera F, Anasetti F, Bellini CM, et al. The influence of the axial, antero-posterior and lateral positions of the center of rotation of a ball-and-socket disc prosthesis on the cervical spine biomechanics. Clin Biomech (Bristol Avon). 2010;25:397–401.
37. Kang H, Park P, La Marca F, et al. Analysis of load sharing on uncovertebral and facet joints at the C5-6 level with implantation of the Bryan, Prestige LP, or ProDisc-C cervical disc prosthesis: an in vivo image-based finite element study. Neurosurg Focus. 2010;28:E9.
38. Ryu KS, Park CK, Jun SC, et al. Radiological changes of the operated and adjacent segments following cervical arthroplasty after a minimum 24-month follow-up: comparison between the Bryan and Prodisc-C devices. J Neurosurg Spine. 2010;13:299–307.
39. Yoganandan N, Purushothaman Y, Choi H, et al. Biomechanical Study of Cervical Disc Arthroplasty Devices Using Finite Element Modeling. J Eng Sci Med Diagn Ther. 2021;4:021004.
40. Mo Z, Li Q, Jia Z, et al. Biomechanical consideration of prosthesis selection in hybrid surgery for bi-level cervical disc degenerative diseases. Eur Spine J. 2017;26:1181–90.
41. Wang Z, Zhao H, Liu JM, et al. Resection or degeneration of uncovertebral joints altered the segmental kinematics and load-sharing pattern of subaxial cervical spine: A biomechanical investigation using a C2-T1 finite element model. J Biomech. 2016;49:2854–62.
42. Hussain M, Natarajan RN, An HS, et al. Patterns of height changes in anterior and posterior cervical disc regions affects the contact loading at posterior facets during moderate and severe disc degeneration: a poroelastic C5-C6 finite element model study. Spine (Phila Pa 1976). 2010;35:E873–881.

43. Hussain M, Natarajan RN, An HS, et al. Reduction in segmental flexibility because of disc degeneration is accompanied by higher changes in facet loads than changes in disc pressure: a poroelastic C5-C6 finite element investigation. Spine J. 2010;10:1069–77.
44. Prado M, Mascoli C, Giambini H. Discectomy decreases facet joint distance and increases the instability of the spine: A finite element study. Comput Biol Med. 2022;143:105278.
45. Volz M, Elmasry S, Jackson AR, et al. Computational Modeling Intervertebral Disc Pathophysiology: A Review. Front Physiol. 2021;12:750668.
46. Garay RS, Solitro GF, Lam KC, et al. Characterization of regional variation of bone mineral density in the geriatric human cervical spine by quantitative computed tomography. PLoS ONE. 2022;17:e0271187.
47. Al-Barghouthi A, Lee S, Solitro GF, et al. Relationships Among Bone Morphological Parameters and Mechanical Properties of Cadaveric Human Vertebral Cancellous Bone. JBMR Plus. 2020;4:e10351.

Publisher's note